

Superplastic Behavior of Friction Stir Processed ZK60 Magnesium Alloy

G. M. Xie^{1,*}, Z. A. Luo¹, Z. Y. Ma², P. Xue² and G. D. Wang¹

¹State Key Laboratory of Rolling and Automation, Northeastern University, Shenyang 110819, P. R. China

²Shenyang National Laboratory for Materials Science, Institute of Metal Research, Chinese Academy of Sciences, Shenyang 110016, P. R. China

Six millimeter thick extruded ZK60 magnesium alloy plate was subjected to friction stir processing (FSP) at 400 rpm and 100 mm/min, producing fine and uniform recrystallized grains with predominant high-angle grain boundaries of 73%. Maximum elongation of 1800% was achieved at a relatively high temperature of 325°C and strain rate of $1 \times 10^{-3} \text{ s}^{-1}$. Grain boundary sliding was identified to be the primary deformation mechanism in the FSP ZK60 alloy by superplastic data analyses and surface morphology observation. The superplastic deformation kinetics of the FSP ZK60 alloy was faster than that of the high-ratio differential speed rolled ZK60 alloy. [doi:10.2320/matertrans.M2011231]

(Received July 28, 2011; Accepted September 27, 2011; Published November 16, 2011)

Keywords: friction stir processing (FSP), magnesium, microstructure, superplasticity

1. Introduction

ZK60 alloy is one of commercial magnesium alloys that exhibit sound mechanical properties. A number of investigations have identified that the excellent superplasticity in the ZK60 alloy could be obtained by the severe plastic deformation methods, such as equal channel angular pressing (ECAP), high ratio differential speed rolling (HRDSR) and isothermal rolling.¹⁻⁶ Figueiredo and Langdon¹ reported an extraordinarily large elongation of 3050% in ECAP ZK60 alloy at 200°C and a strain rate of $1 \times 10^{-4} \text{ s}^{-1}$. Moreover, Lapovok *et al.*² achieved a large elongation of 2040% in ECAP ZK60 alloy at 220°C and a strain rate of $3 \times 10^{-4} \text{ s}^{-1}$. Galiyev and Kaibyshev³ reported that isothermal rolled ZK60 alloy exhibited a maximum elongation of 1330% at 250°C and $1.4 \times 10^{-4} \text{ s}^{-1}$. The superplasticity of ECAP and isothermal rolled ZK60 alloy was usually obtained at a relatively low temperature and strain rate. This should be due to the poor thermal stability of the as-processed ZK60 alloy, where a number of low angle non-equilibrium grain boundaries were usually observed.⁴ Generally speaking, improving the thermal stability of ZK60 alloy can increase the strain rate of superplastic deformation. Kim *et al.*^{5,6} reported that the HRDSR ZK60 alloy exhibited a maximum elongation of 926% at relatively high temperature of 280°C and a high strain rate of $1 \times 10^{-2} \text{ s}^{-1}$. In the HRDSR ZK60 alloy, an excellent thermal stability was achieved due to the enhanced fraction of high angle grain boundaries (HAGBs).⁶

Friction stir processing (FSP) has been developed as a solid-state processing technique, based on the concept of friction stir welding (FSW).⁷ FSP resulted in the generation of a fine-grained structure with high fraction HAGBs in the stir zone (SZ) due to the dynamic recrystallization process. As a thermo-mechanical processing method, FSP has some special advantages for commercial applications of superplasticity: (a) FSP is a simple one-pass processing method; (b) Unrequired preheating avoids surface oxidation of a sample and saves energy; (c) FSP leads the SZ to a fine grain structure with high fraction HAGBs, which is favorable for

superplastic deformation dominated by grain boundary sliding (GBS).

At the present time, the investigation on the FSP aluminum alloy was widely reported, and the high strain rate superplasticity could be easily achieved in FSP fine-grained aluminum alloy due to the high fraction HAGBs.⁷ However, the studies on the superplastic deformation of FSP magnesium alloys are relatively limited.⁸⁻¹¹ Some of the authors^{8,9} reported that the superplastic deformation kinetics of FSP Mg-Zn-Y-Zr alloys were significantly faster than that of ECAP AZ91 alloy, and a maximum elongation of 1110% was achieved at 450°C and a high strain rate of $1 \times 10^{-2} \text{ s}^{-1}$ with predominant HAGBs of 91%. Furthermore, Cavaliere and De Marco^{10,11} also reported that good superplasticity was achieved in FSP AZ91 and AM60 alloys with the optimum strain rates in the range of 10^{-4} to 10^{-3} s^{-1} .

To the best of our knowledge, no study on superplastic behavior of FSP ZK60 alloy has been reported so far. So it is very interesting to demonstrate whether excellent superplasticity can be obtained in fine-grained ZK60 alloy via FSP. In the present work, we produced fine-grained ZK60 alloy via FSP and investigated the superplastic deformation behavior at different temperature and strain rates. Besides, the superplastic deformation mechanism was also analyzed in detail.

2. Experimental Procedure

6 mm thick ZK60 (Mg-6.0Zn-0.6Zr, mass%) extruded plate was subjected to FSP at a rotation rate of 400 rpm and a traverse speed of 100 mm/min. A steel tool with a concave shoulder 20 mm in diameter and a threaded conical pin 6 mm in root diameter and 5.7 mm in length was used. Microstructural characterization was performed by optical microscopy (OM), transmission electron microscopy (TEM) and electron backscatter diffraction (EBSD). The average grain size was measured by the mean linear intercept method.

Mini tensile specimens of 2.5 mm gauge length with 1.4 mm in width and 1.0 mm in thickness (corner radius is 1.5 mm) were electrodischarge machined perpendicular to the SZ of FSP sample from the central portion of SZ. The

*Corresponding author, E-mail: xiegm@ral.neu.edu.cn

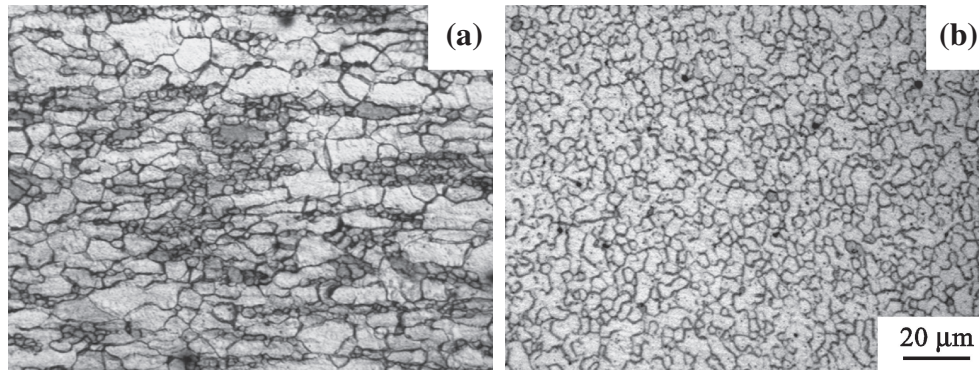


Fig. 1 OM micrographs showing grain structures: (a) as-extruded BM, (b) SZ of FSP sample.

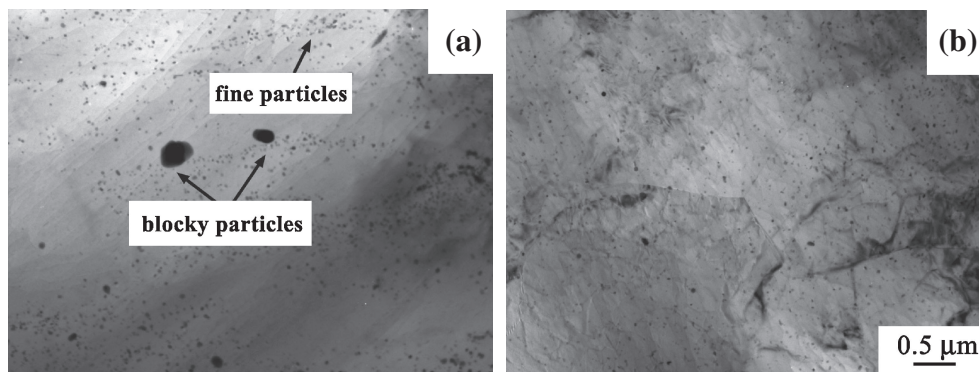


Fig. 2 TEM images showing second phase particles distribution: (a) as-extruded BM, (b) SZ of FSP sample.

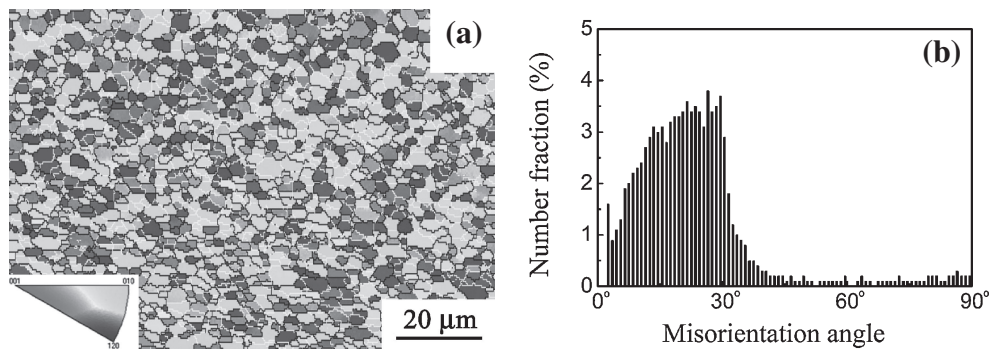


Fig. 3 (a) EBSD map and (b) grain boundary misorientation angle distribution in SZ of FSP ZK60 alloy.

specimens were subsequently ground and polished before the tensile test. Each specimen was fastened in the tensile testing apparatus when the furnace was heated to the selected testing temperature, then held for 15 min to achieve thermal equilibrium prior to the tensile test. The surface characteristic of the failed samples was characterized by scanning electron microscopy (SEM).

3. Results and Discussion

The microstructures of the as-extruded base material (BM) and the SZ of FSP ZK60 alloy are shown in Fig. 1. The BM exhibited a typical strip-like structure which contained coarse and non-uniform grains (Fig. 1(a)). However, intense plastic

deformation and frictional heating during FSP resulted in the generation of uniform recrystallized fine grains in the SZ (Fig. 1(b)), and the average grain size of the SZ (about 3 μm) was significantly smaller than that of the BM (about 8.5 μm).

Figures 2(a) and 2(b) show the bright-field TEM images of the second phase particles in the BM and SZ, respectively. Currently, a mount of studies on second phase in the ZK60 alloy have been reported.^{12–14} He *et al.*¹² indicated that the large blocky particles and fine particles consisted of β'' (MgZn_2) phase and β' (MgZn) phase, respectively, in ECAP ZK60 alloy. Further, in our previous study, we also found that FSW resulted in the dissolution of β'' phase in the SZ of ZK60 alloy.¹³ Therefore, the large dark blocky particles

in the BM as indicated by the arrows in Fig. 2(a) consisted of β'' phase, while the fine particles distributed homogeneously in the SZ of the FSP ZK60 alloy should be β' precipitates.

Figure 3(a) shows the microstructure of the FSP ZK60 alloy obtained by EBSD mapping. It is clear that the microstructure was characterized by equiaxed grains, which is in accord with the OM observations. The distribution of the grain boundary (GB) misorientation angle in the SZ of the FSP ZK60 alloy was shown in Fig. 3(b), where the HAGBs (grain boundary misorientation angle $\geq 15^\circ$) and low-angle grain boundaries (grain boundary misorientation angle $< 15^\circ$) were identified by black and white lines, respectively. From the distribution of GB misorientation angle, a broad peak in the angular range of $5\text{--}30^\circ$ can be observed clearly. This should be associated the prismatic slip which provides a lattice rotation around the $\langle 0001 \rangle$ axis.^{14,15} Due to limitations imposed by the symmetry of the HCP crystal structure, the maximal rotation angle measured around the $\langle 0001 \rangle$ axis is limited to 30° . Considering all GBs with misorientation angles $> 2^\circ$, the HAGBs comprised about 73% of the total GB length in the SZ of the present FSP ZK60 alloy. Mironov *et al.*¹⁴ reported that the fraction HAGBs measured by EBSD was 65% in the ZK60 alloy FS-welded at 600 rpm and 100 mm/min by a tool with shoulder diameter of 14 mm.

Figure 4(a) shows the variation of elongation versus initial strain rate for the FSP ZK60 alloy at 300, 325 and 350°C, respectively. At 300°C, a maximum elongation of 1400% was obtained at the optimum strain rate of $3 \times 10^{-4} \text{ s}^{-1}$. However, at 325 and 350°C, the optimum strain rate for maximum elongation was shifted to a higher value of

$1 \times 10^{-3} \text{ s}^{-1}$. The largest elongation of 1800% was achieved at 325°C and a relatively high strain rate of $1 \times 10^{-3} \text{ s}^{-1}$ in this study. For the HRDSR ZK60 alloy, a maximum elongation of 926% was achieved at 280°C and an optimum strain rate of $1 \times 10^{-2} \text{ s}^{-1}$,⁶ while the ECAP ZK60 alloy showed a maximum elongation of 3050% at 200°C and $1 \times 10^{-4} \text{ s}^{-1}$.¹ Clearly, the testing temperature for the superplastic deformation of FSP ZK60 alloy is higher than that of ECAP and HRDSR ZK60 alloys. This indicated that the FSP ZK60 alloy exhibited excellent thermal stability. Figure 4(b) shows the variation of flow stress versus the initial strain rate for the FSP ZK60 alloy. The strain rate sensitivity exponent m of the FSP ZK60 alloy is approximately 0.5 throughout the investigated strain rate range of $3 \times 10^{-4}\text{--}1 \times 10^{-2} \text{ s}^{-1}$. The m value of about 0.5 in the present FSP ZK60 alloy suggested that the GBS should be the main deformation mechanism.¹⁶

Figure 5(a) displays the untested and failed samples for FSP ZK60 alloy deformed to failure at 325°C for different initial strain rates. The failed specimens showed neck-free elongation which was the typical characteristic of superplastic flow. The surface morphology of the FSP ZK60 alloy deformed at 325°C and $1 \times 10^{-3} \text{ s}^{-1}$ to failure was subjected to SEM examination, and the evidence of extensive GBS was revealed, as shown in Fig. 5(b). It is attributed to the occurrence of the high fraction HAGBs promoting the GBS.

It is well known that the high fraction HAGBs could enhance the thermal stability, which is beneficial to enhance superplasticity.⁴ Compared to the FSP ZK60 alloy which contained 73% HAGBs, HRDSR ZK60 alloy exhibited lower fraction HAGBs (43–52%).⁶ Therefore, FSP ZK60 alloy showed higher superplastic deformation temperature which would change the superplastic behavior. Compared to ECAP magnesium alloy, more favorite microstructure for superplastic deformation kinetics was obtained in FSP Mg-Zn-Y-Zr alloy.⁸

The classic equation of superplastic deformation behavior of fine-grained ($< 10 \mu\text{m}$) magnesium alloys with GBS as main deformation mechanism is:¹⁷

$$\dot{\epsilon} = 2 \times 10^5 \left(\frac{D_0 G b}{kT} \right) \exp \left(- \frac{92000}{RT} \right) \left(\frac{b}{d} \right)^3 \left(\frac{\sigma - \sigma_0}{G} \right)^2 \quad (1)$$

Where $\dot{\epsilon}$ is the strain rate, D_0 is the pre-exponential constant for diffusivity, G is the shear modulus, b is the

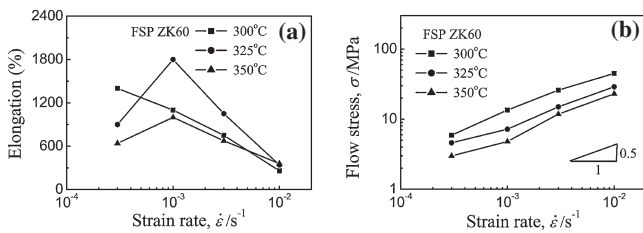


Fig. 4 Variation of initial strain rate versus (a) elongation and (b) flow stress for FSP ZK60 alloy.

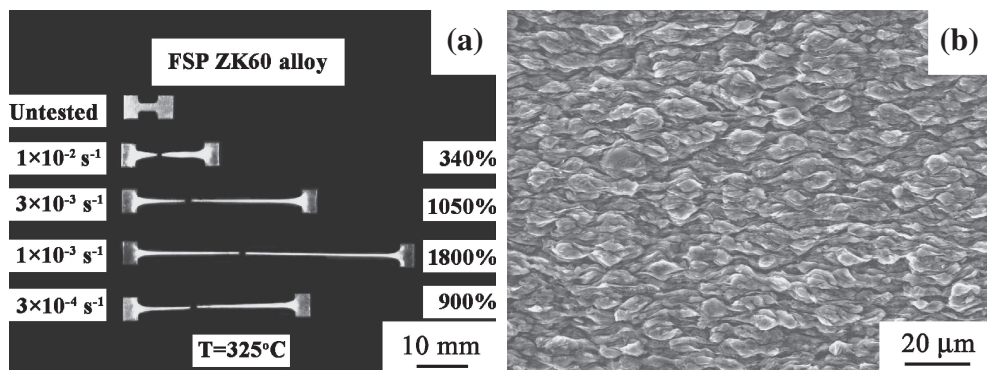


Fig. 5 (a) Macrographs of untested and failed tensile specimens; (b) surface morphology of the specimen deformed at 325°C and $1 \times 10^{-3} \text{ s}^{-1}$.

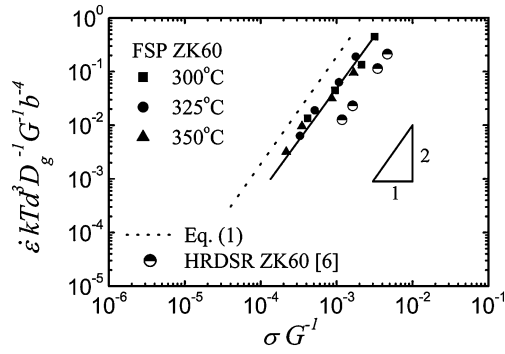


Fig. 6 Variation of $\dot{\epsilon} k T d^3 D_g^{-1} G^{-1} b^{-4}$ with normalized effective stress σG^{-1} for FSP and HRDSR ZK60 alloys.

Burger's vector, k is the Boltzmann constant, T is the absolute temperature, R is the gas constant, d is the grain size, σ is the flow stress, and σ_0 is the threshold stress. Galiyev and Kaibyshev¹⁸⁾ reported the precipitates in Mg-Zn-Zr alloy exhibited low thermal stability and were in solution state above 300°C. Therefore, under the relatively high deformation temperature range (300–350°C), the precipitates in the present FSP ZK60 alloy do not influence on the superplastic deformation, thus no threshold-type deformation behavior is expected.

The superplastic data from the FSP and HRDSR ZK60 alloys were plotted in Fig. 6 as $\dot{\epsilon} k T d^3 D_g^{-1} G^{-1} b^{-4}$ vs σG^{-1} (D_g is the grain boundary diffusion coefficient, $D_g = D_0 \exp(-\frac{92000}{RT})$). For comparison, a dashed line predicted by eq. (1) was also included. It is noted that the slope of the dashed line predicted by eq. (1) and the fitted solid line by superplastic data of FSP ZK60 alloy are almost equal. So, the activation energy of FSP ZK60 alloy is similar to that for magnesium grain-boundary self-diffusion (92000 J/mol). Moreover, the superplastic deformation kinetics of the FSP ZK60 alloy is significantly faster than that of HRDSR ZK60 alloy. That is to say, more favorite microstructure for superplastic deformation kinetics was achieved in the FSP ZK60 alloy compared to HRDSR ZK60 alloy.

Compared to the HRDSR ZK60 alloy, although the FSP ZK60 alloy did not exhibit high strain rate superplasticity, the deformation kinetics was faster than that of HRDSR ZK60 alloy. This should be due to the relatively high fraction HAGBs in the present FSP ZK60 alloy. Generally, the fraction HAGBs for magnesium alloy can be increased further by changing FSP parameters, such as rotation rate, traverse speed, and tool size. Therefore, higher strain rate superplasticity can be achieved in FSP ZK60 alloy via changing FSP parameters.

4. Conclusions

FSP resulted in the fine grains of about 3 μm with predominant HAGBs of about 73% and uniformly distributed second phase particles in ZK60 alloy. The maximum elongation of 1800% was obtained in FSP ZK60 alloy at a relatively high temperature of 325°C and strain rate of $1 \times 10^{-3} \text{ s}^{-1}$, indicating that the excellent thermal stability was achieved in FSP ZK60 alloy. GBS was the primary deformation mechanism. The superplastic deformation kinetics of the FSP ZK60 alloy was faster than that of HRDSR ZK60 alloy.

Acknowledgements

This work was supported by National Natural Science Foundation of China (No. 51001023) and Fundamental Research Funds for the Chinese Central Universities N090307003.

REFERENCES

- 1) R. B. Figueiredo and T. G. Langdon: *Adv. Eng. Mater.* **10** (2008) 37–40.
- 2) R. Lapovok, P. F. Thomson, R. Cottam and Y. Estrin: *Mater. Sci. Eng. A* **410–411** (2005) 390–393.
- 3) A. Galiyev and R. Kaibyshev: *Scr. Mater.* **51** (2004) 89–93.
- 4) H. Watanabe, T. Mukai, K. Ishikawa and K. Higashi: *Scr. Mater.* **46** (2002) 851–856.
- 5) W. J. Kim, M. J. Kim and J. Y. Wang: *Mater. Sci. Eng. A* **527** (2009) 322–327.
- 6) W. J. Kim, B. H. Lee, J. B. Lee, M. J. Lee and Y. B. Park: *Scr. Mater.* **63** (2010) 772–775.
- 7) R. S. Mishra and Z. Y. Ma: *Mater. Sci. Eng. R* **50** (2005) 1–78.
- 8) G. M. Xie, Z. Y. Ma, L. Geng and R. S. Chen: *J. Mater. Res.* **23** (2008) 1207–1213.
- 9) Q. Yang, B. L. Xiao, Z. Y. Ma and R. S. Chen: *Scr. Mater.* **65** (2011) 335–338.
- 10) P. Cavaliere and P. P. De Marco: *Mater. Sci. Eng. A* **462** (2007) 393–397.
- 11) P. Cavaliere and P. P. De Marco: *J. Mater. Process. Technol.* **184** (2007) 77–83.
- 12) Y. He, Q. Pan, Y. Qin, X. Liu, W. Li, Y. Chiu and J. J. J. Chen: *J. Alloy. Compd.* **492** (2010) 605–610.
- 13) G. M. Xie, Z. Y. Ma and L. Geng: *Mater. Sci. Eng. A* **486** (2008) 49–55.
- 14) S. Mironov, Y. Motohashi, T. Ito, A. Goloborodko, K. Funami and R. Kaibyshev: *Mater. Trans.* **48** (2007) 3140–3148.
- 15) U. F. H. R. Suhuddin, S. Mironov, Y. S. Sato, H. Kokawa and C. W. Lee: *Acta Mater.* **57** (2009) 5406–5418.
- 16) T. G. Langdon: *Acta Metall. Mater.* **42** (1994) 2437–2443.
- 17) H. Watanabe, H. Tsutsui, T. Mukai and T. Aizawa: *Mater. Japan* **39** (2000) 347–350.
- 18) A. M. Galiyev and R. O. Kaibyshev: A supplemental Volume to Superplasticity and Superplastic Forming, ed. by A. K. Ghosh and T. R. Bieler, (The Minerals, Metals & Materials Society, Warrendale PA, 1998) pp. 20–29.